Materials Transactions, Vol. 45, No. 7 (2004) pp. 2389 to 2394
©2004 The Japan Institute of Metals

Effect of ARB Cycle Number on Cell Morphology of Closed-Cell Al-Si Alloy Foam

Koichi Kitazono[1], Seiji Nishizawa[2]*, Eiichi Sato[1] and Tetsuichi Motegi[2]

[1]*Institute of Space and Astronautical Science, Japan Aerospace Exploration Agency, Sagamihara 229-8510, Japan*
[2]*Faculty of Engineering, Chiba Institute of Technology, Narashino 275-8588, Japan*

Closed-cell Al-Si alloy foam was produced from two bulk alloy strips. Preform sheet containing titanium hydride (TiH_2) particles was first manufactured through accumulative roll-bonding (ARB) processing. Large ARB cycle number was effective to achieve uniform distribution of the TiH_2 particles in the Al-Si matrix. Following high temperature foaming tests revealed that high porosity and small pore size can be obtained from the preform prepared through large cycle number. These results indicate that a suitable ARB processing condition enables to optimize the cell microstructure of the metal foams.

(Received March 5, 2004; Accepted May 11, 2004)

Keywords: *foam, cell morphology, accumulative roll-bonding, porous material, aluminum-silicon alloy*

1. Introduction

Many researchers and engineers are interested in metal foams in recent years because of their low density, high specific strength, high damping capacity, high energy absorption, high sound absorption and high electromagnetic shielding properties.[1)] They offer benefits for automotive, aerospace, naval and other industrial applications. Morphology of the metal foams is classified into two types: open-cell metal foam having interconnected pores and closed-cell metal foam having isolated pores. Though the former has a potential as filters and heat exchangers, their mechanical properties are inferior to those of the latter. Thus, the present study focuses on closed-cell aluminum foams as lightweight structural applications.

Two major manufacturing methods of the closed-cell aluminum foams are melt route[2–4)] and powder metallurgical (P/M) route.[5–7)] The former enable to manufacture a large aluminum foam ingot using a special casting system. Canadian company Cymat[2)] and Japanese company Shinko-Wire[3)] have developed closed-cell foams by gas injection and blowing agent methods, respectively. However, there is little room left for improving mechanical properties by adding alloying elements or dispersing strengthening particles because of their narrow foaming and solidification conditions.[8)] The latter have advantages of near net-shape and flexibility in alloy choice. In the typical P/M route, powder of aluminum metal or alloy is first blended with appropriate blowing agent particles and compacted by conventional methods to produce a dense composite material which is called "precursor". Heating the precursor to just below its melting point turns the matrix into a viscous mass. It simultaneously causes the blowing agent to decompose. Consequently, the precursor expands and forms into a closed-cell aluminum foam. The disadvantages of the P/M route are relatively expensive metal powder and the difficulty to make large volume parts. Large compacted precursor often contains small pores and cracks which often hinder the following foaming process.[9)]

Recently, the authors proposed a new manufacturing route

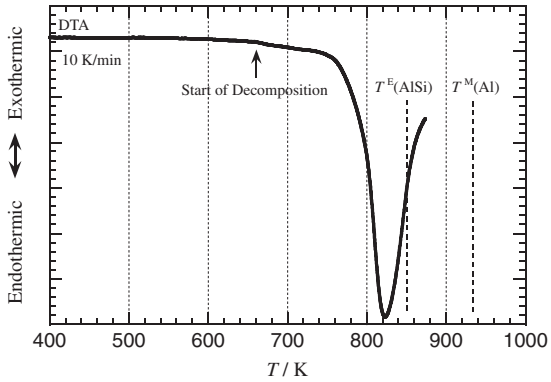


Fig. 1 DTA curve of free TiH_2 particles in argon. Two broken lines show melting point of pure aluminum, T^M, and eutectic point of Al-Si binary alloy, T^E.

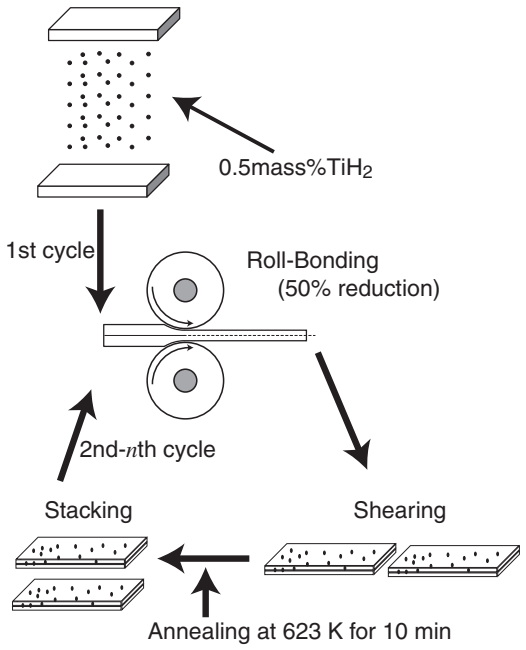


Fig. 2 Schematic illustration of the manufacturing process of a preform sheet through ARB process.

*Graduate Student, Chiba Institute of Technology

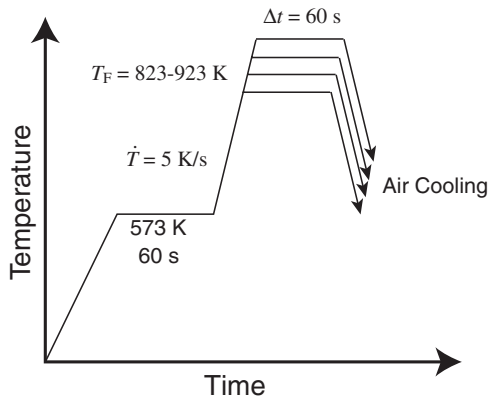


Fig. 3 Temperature profile during the foaming test by an infrared image furnace. Foaming temperature, T_F, corresponds to the TC temperature in the furnace.

of closed-cell metal foams using neither metal melt nor powder, which is classified into a bulk route.[10] A dense aluminum matrix composite sheet containing blowing agent particles, which is called "preform", is first manufactured by a modified accumulative roll-bonding (ARB) process.[11] Original ARB process is one of intense plastic straining processes to produce ultra-fine crystal grains and has been applied on many metals and alloys.[12] In the following, the preform is heated to near its melting point and foams into a closed-cell foam. This foaming stage is the same as that of P/M route.

Many investigators have aimed to control the cell morphology in order to produce high performance metal foams. The porosity and the microstructure of the closed-cell aluminum foams depend not only on the foaming condition but on the microstructure of the preform. Therefore, the ARB processing condition directly affects the final properties of the aluminum foam. In the present study, we experimentally examine the effects of the ARB processing condition on the microstructure of the preform and the cell morphology of the aluminum foam. Hypoeutectic or near eutectic Al-Si alloy powder has been generally used in P/M route because of its low melting point and good foamability.[13] Here, we also use near eutectic Al-Si alloy sheets which are mainly used as a brazing sheet.[14]

2. Experimental Procedure

Hot-rolled 4045 Al-Si alloy sheets with 3 mm thickness were specially supplied by Sumitomo Light Metals Industries, Ltd. for this study. The chemical composition is listed in Table 1. The optical microstructure showed fine silicon particles dispersed in the aluminum matrix. Titanium hydride (TiH_2) particles were used as a blowing agent because they are suitable for aluminum system and widely used in both melt and P/M foaming processes. Differential thermal analysis (DTA) curve of TiH_2 particles was measured in Ar atmosphere (Fig. 1). Free TiH_2 particles showed that decomposition starts at 653 K and continues up to 820 K. It is noted that this result is valid only for free powders and depends on the heating rate and the environmental atmosphere. The important point is that the ARB processing must be carried out below the decomposition temperature of the TiH_2 powder.

Table 1 Chemical composition of 4045 Al-Si alloy sheets (mass%).

Si	Fe	Cu	Mn	Mg	Zn	Ti	Al
10.52	0.20	0.03	0.01	0.02	0.01	0.03	Bal.

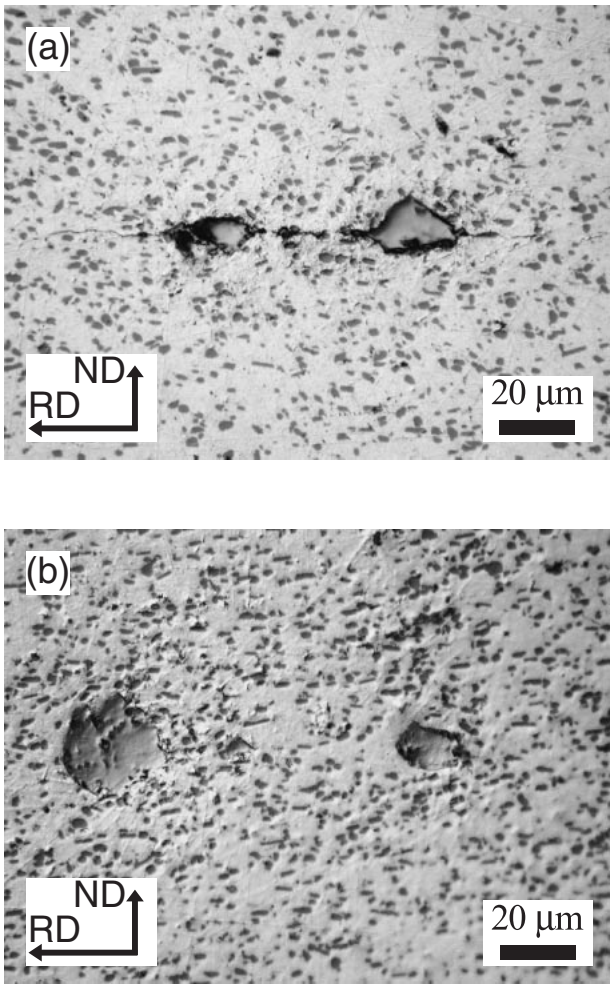


Fig. 4 Optical micrographs of the typical preform sheet during the ARB processing. (a) and (b) are the bonding boundary just after the 50% roll-bonding and after heat treatment at 623 K for 10 min, respectively.

Foamable preform sheet is manufactured by ARB method which is schematically illustrated in Fig. 2. Two Al-Si strips with 30 mm width and 300 mm length were prepared as starting materials. All strips were annealed for 60 min at 623 K in atmosphere. The bonding interfaces were cleaned by acetone and polished by a stainless steel wire brush. Before stacking the strips, 0.5 mass% (0.3 vol%) TiH_2 particles less than 45 μm in size were uniformly sprinkled on the bonding interface. After fastening the strips by small stainless steel clips, they were roll-bonded with draft percentage of 50% in one cycle at 523 K. Here, roll-bonding was carried out with no lubricant using two-high rolling mills with 252 mm diameter. In order to improve the bonding strength and to reduce the hardness of the matrix, the strips were annealed at 623 K for 10 min after each roll-bonding. The roll-bonded strip was cut into two strips by a shearing machine. These

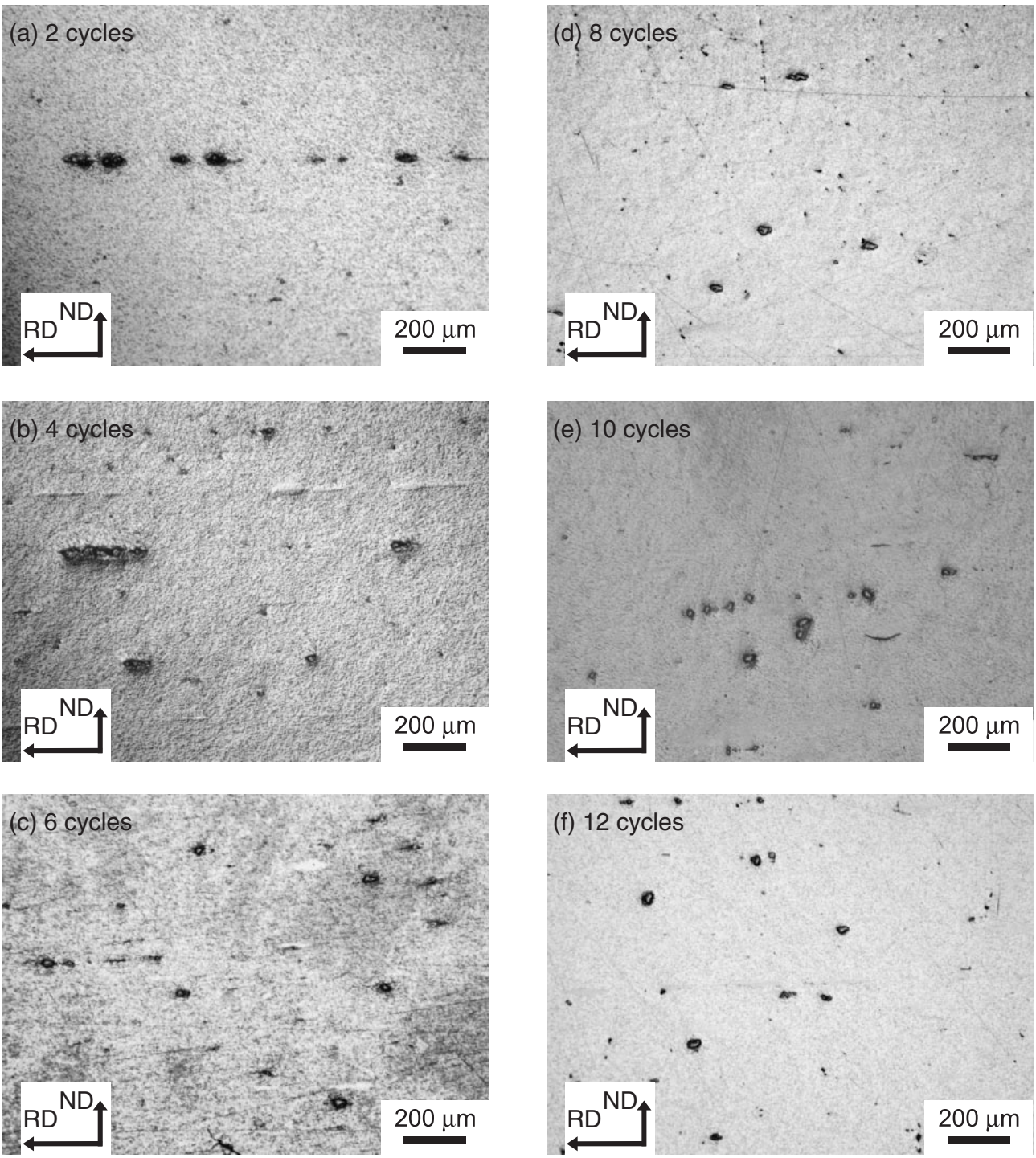


Fig. 5 Optical micrographs of 4045 Al-Si alloy preform after (a) 2, (b) 4, (c) 6, (d) 8, (e) 10 and (f) 12 ARB cycles. Polygonal TiH_2 particles were gradually dispersed in the Al-Si matrix with increasing in the ARB cycle number.

strips were used as the starting material for the second cycle of roll-bonding. It is noted that the TiH_2 particles were only sprinkled at the beginning of the first cycle.

Six kinds of preform sheets were produced through 2, 4, 6, 8, 10 and 12 ARB cycles. After microstructural observation of the preforms, they were machined into 15 mm × 15 mm square specimens. High temperature foaming test was performed in atmosphere using an infrared image furnace. The furnace temperature was measured and controlled by K-type thermocouple (TC) which was positioned at the bottom of the specimen. The real temperature of the specimen was 10~20 K higher than the value of TC. Temperature profiles used in the present foaming test are illustrated in Fig. 3. After isothermal holding at 573 K for 60 s for stabilizing the image furnace, the specimen is heated at the fixed heating rate of 5 K/s. When the TC temperature achieved at the foaming temperature, T_F, heating is stopped and the specimen is held isothermally for 60 s. At last, the specimen is cooled down to the room temperature.

The macroscopic density, ρ^*, of the foamed specimen including skins is evaluated by Archimedes' principle. Then, the porosity, p, is calculated as

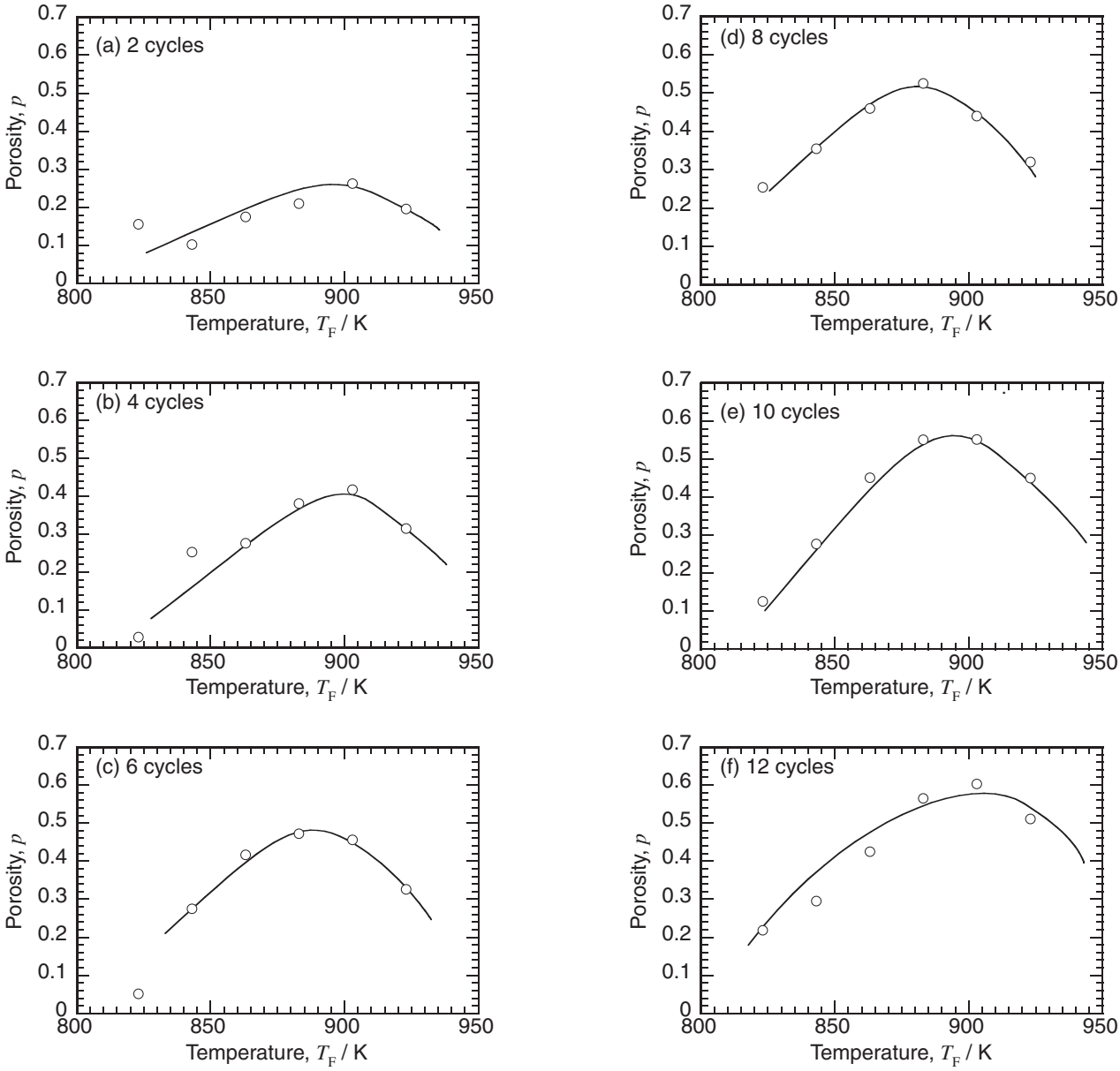


Fig. 6 Porosities of the 6 specimens foamed under various foaming temperatures against the foaming temperature.

$$p = 1 - (\rho^*/\rho_S), \tag{1}$$

where ρ_S is the density of the bulk 4045 alloy ($\rho_S = 2.68 \times 10^3$ kg/m^3) and the gas density in the pores is neglected. The cell morphology was observed by a stereoscope after cutting the foam by an electro discharge machine (EDM).

3. Results

3.1 ARB processing

The roll-bonded strip was annealed at 623 K for 10 min in order to enhance the bonding strength and to reduce the matrix hardness. Typical microstructures of the bonding boundary before and after the annealing were observed by optical microscope (Fig. 4). In addition, the hardness of the Al-Si matrix was measured through Vickers hardness tests. Polygonal TiH_2 particles were embedded at the bonding boundary. Clear boundary lines appeared in the pre-annealed preform (Fig. 4(a)) and its matrix hardness was high (60 Hv). On the other hand, most of the bonding lines disappeared and the matrix hardness decreased (38 Hv) in the annealed stip (Fig. 4(b)). Therefore, the heat treatment is effective to improve the bonding strength and reduce the strain hardening.

The microstructures of the six kinds of preform sheets were observed from the transverse direction (TD) (Fig. 5). After one and two ARB cycles, the TiH_2 particles exist at the bonding boundaries parallel to the rolling direction (RD). However, the TiH_2 particles were gradually separated and dispersed in the matrix with increasing the ARB cycle. The sizes of TiH_2 particles were slightly decreased during the ARB processing.

3.2 High temperature foaming

The six kinds of preform specimens were foamed under various foaming temperatures. The porosity calculated from

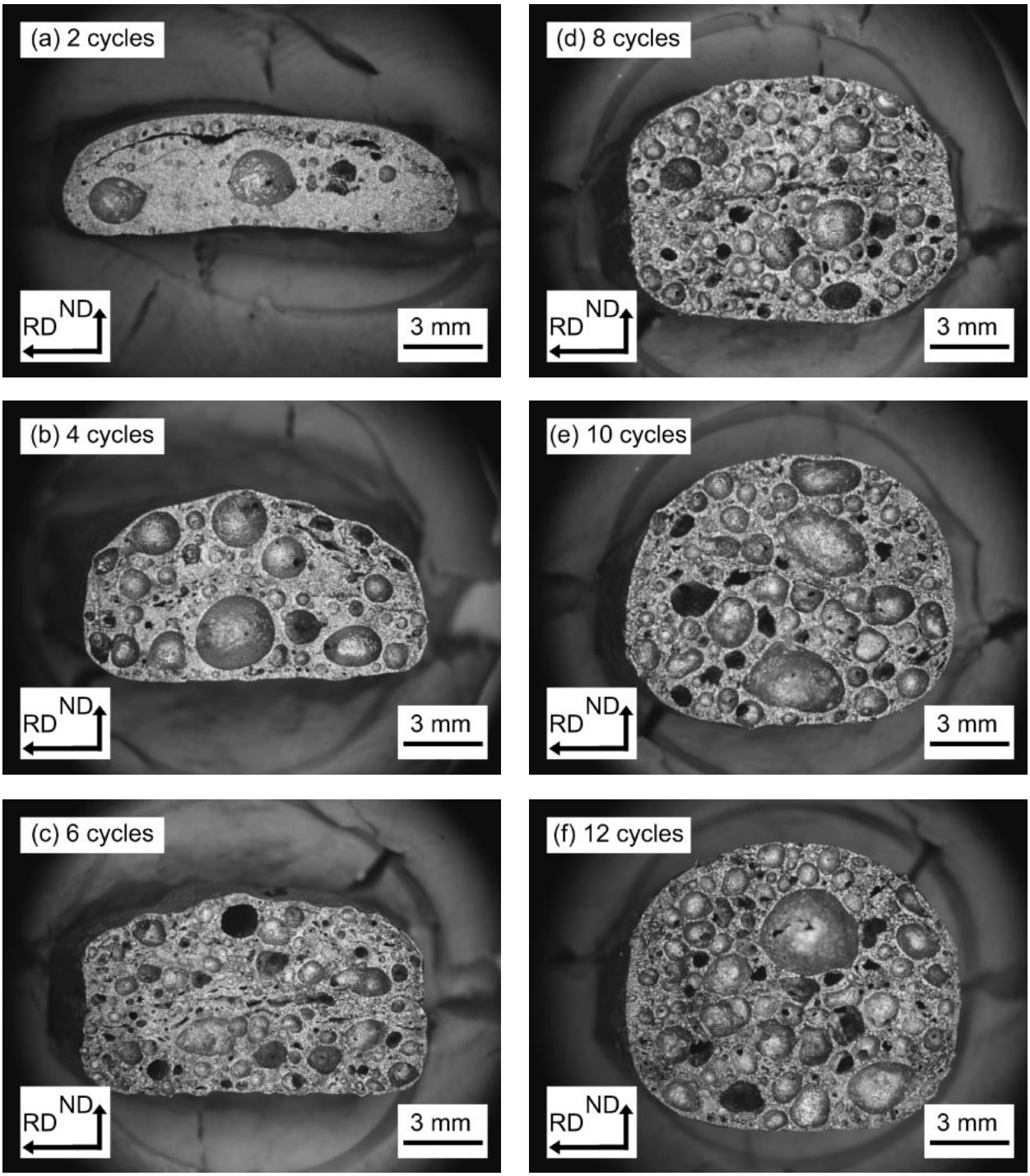


Fig. 7 Photographs of the cross sections of the foamed specimens. Pore size decreased with increasing in the ARB cycle number.

eq. (1) was plotted against the foaming temperature (Fig. 6). In all specimens, the porosity was increased with increasing the foaming temperature, however, it decreased at higher temperature ranges because of cell coalescence and gas escape. The maximum porosities after 2, 4, 6, 8, 10 and 12 ARB cycles are 0.26, 0.42, 0.47, 0.53, 0.55 and 0.60% obtained by the foaming tests at 903, 903, 883, 883, 903 and 903 K, respectively.

The foamed specimens which showed maximum porosity at respective temperatures were cut by EDM and the transverse sections were observed (Fig. 7). The preferential volume expansion occurred parallel to the nominal direction (ND). Though the foamed specimen after two ARB cycles contained a few large spherical pores, the number of pores increased with increasing the cycle number. On the other hand, the average pore size decreased with increasing the cycle number. Similar cell morphologies were observed in the foamed specimens over six ARB cycles.

4. Discussion

Geometrical change of the preform microstructure during

Table 2 Geometrical changes in aluminum and TiH_2 layers during the ARB processing by 50% reduction per cycle.

ARB cycle number	1	2	3	…	7	…	n
Number of Al layers	2	4	8	…	128	…	2^n
Thickness of Al layers/μm	1500	750	375	…	23.4	…	$3000 \cdot 2^{-n}$
Number of TiH_2 layers	1	2	4	…	64	…	2^{n-1}

the ARB processing is simply calculated and is listed in Table 2. Numbers of Al layers, thickness of Al layers and number of TiH_2 layers are expressed as a function of the ARB cycle number, n. The thickness of Al layyers exponentially decrease with increasing the cycle number. Over seven ARB cycles, it becomes smaller than the initial size of TiH_2 particles. Therefore, it is suggested that TiH_2 particles are uniformly dispersed in the continuous Al-Si matrix over seven ARB cycles. This is experimentally verified in Fig. 5: though we can identify the TiH_2 layers in the cross sections of the preforms after two and four ARB cycles, we cannot find them over six ARB cycles.

Porosity and microstructure strongly effect on physical properties of metal foams. Generally, many industrial applications require high porosity to reduce the weight of the parts. In order to clarify the effect of the ARB cycle number on the porosity, the maximum porosity was plotted against the cycle number in Fig. 8. The porosity monotonously increased with increasing the cycle number at each temperature. Therefore, large cycle number is obviously effective to increase the porosity, because the uniform distribution of the TiH_2 particles in the preform restricts the coalescence of the pores. Insufficient TiH_2 distribution due to the small cycle number will accelerate the coalescence of the pores.

The maximum porosity of the present Al-Si foams was 0.60 which was higher than previously reported pure aluminum foam produced by the ARB processing.[10] This is obviously due to the superior foamability of Al-Si matrix. On the other hand, Baumgärtner *et al.*[7] described that typical porosities of P/M aluminum foams including the skins range from 0.7 to 0.85, which is slightly higher than the present maximum porosity. This is probably due to insufficient optimization of the high temperature foaming condition. Controlling the specimen temperature during the foaming stage is more difficult than conventional heat treatment because the specimen expands and changes its shape. We should find out an ideal foaming temperature condition according to the size, shape and thermal property of the preforms.

5. Conclusions

The ARB processing is a new manufacturing method to make closed-cell metal foams from bulk metal sheets. In this study, closed-cell Al-Si alloy foam was successfully produced from bulk 4045 alloy sheets. The maximum porosity was 0.60 which was higher than that of pure aluminum foam produced by the same ARB processing method. Increasing ARB cycle number was effective to achieve uniformly dispersion of TiH_2 particles in the Al-Si matrix. The manufactured preforms were annealed at various foaming temperatures. The maximum porosity increased with increasing the cycle number. On the other hand, an average pore size decreased with increasing the cycle number. Thus, we conclude that large cycle number is effective to produce high quality metal foams.

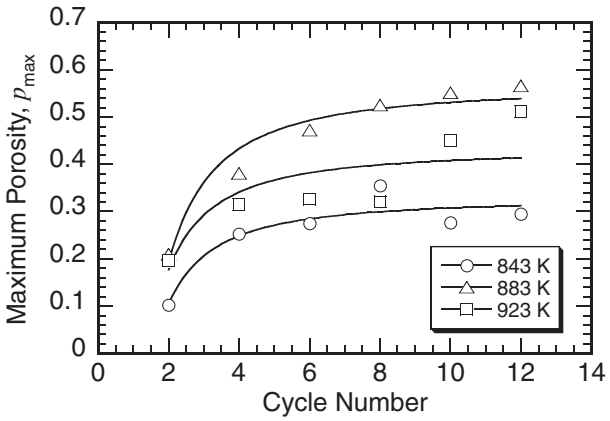


Fig. 8 Maximum porosities after the foaming tests at 843, 883 and 923 K against the ARB cycle number.

Acknowledgments

This study was supported in part by Grants-in-Aid for Scientific Research from the Japan Society for the Promotion of Science. The authors thank Sumitomo Light Metals Industries, Ltd. for providing the materials. The authors also thank Mr. Y. Kikuchi, Tokyo Metropolitan Institute of Technology, for his helpful experimental supports.

REFERENCES

1) J. Banhart: Prog. Mater. Sci. **46** (2001) 559–632.
2) O. Prakash, H. Sang and J. D. Embury: Mater. Sci. Eng. **A199** (1995) 195–203.
3) S. Akiyama, H. Ueno, K. Imagawa, A. Kitahara, S. Nagata, K. Morimoto, T. Nishikawa and M. Itoh: US Patent (1987) 4713277.
4) A. E. Simone and L. J. Gibson: Acta Mater. **46** (1998) 3109–3123.
5) J. Baumeister: US Patent (1992) 5151246.
6) C. Körner, F. Berger, M. Arnold, C. Stadelmann and R. F. Singer: Mater. Sci. Tech. **16** (2000) 781–784.
7) F. Baumgärtner, I. Duarte and J. Banhart: Adv. Eng. Mater. **2** (2000) 168–174.
8) T. Miyoshi, S. Hara, T. Mukai and K. Higashi: Mater. Trans. **42** (2001) 2118–2123.
9) A. R. Kennedy: Powder Metallurgy **45** (2002) 75–79.
10) K. Kitazono, E. Sato and K. Kuribayashi: Scr. Mater. **50** (2004) 495–498.
11) Y. Saito, H. Utsunomiya, N. Tsuji and T. Sakai: Acta Mater. **47** (1999) 579–583.
12) N. Tsuji, Y. Saito, S.-H. Lee and Y. Minamino: Adv. Eng. Mater. **5** (2003) 338–344.
13) I. Duarte and J. Banhart: Acta Mater. **48** (2000) 2349–2362.
14) J. S. Yoon, S. H. Lee and M. S. Kim: J. Mater. Proc. Tech. **111** (2001) 85–89.